D-HAZY: A DATASET TO EVALUATE QUANTITATIVELY DEHAZING ALGORITHMS

Cosmin Ancuti [†*], *Codruta O. Ancuti* [‡*] *and Christophe De Vleeschouwer* [†]

[†] ICTEAM, Universite Catholique de Louvain, Belgium
[‡] Computer Vision and Robotics Group, University of Girona, Spain
[*] MEO, Universitatea Politehnica Timisoara, Romania

ABSTRACT

Dehazing is an image enhancing technique that emerged in the recent years. Despite of its importance there is no dataset to quantitatively evaluate such techniques. In this paper we introduce a dataset that contains 1400+ pairs of images with ground truth reference images and hazy images of the same scene. Since due to the variation of illumination conditions recording such images is not feasible, we built a dataset by synthesizing haze in real images of complex scenes. Our dataset, called **D-HAZY**, is built on the Middelbury [1] and NYU Depth [2] datasets that provide images of various scenes and their corresponding depth maps. Due to the fact that in a hazy medium the scene radiance is attenuated with the distance, based on the depth information and using the physical model of a hazy medium we are able to create a corresponding hazy scene with high fidelity. Finally, using D-HAZY dataset, we perform a comprehensive quantitative evaluation of several state of the art single-image dehazing techniques.

Index Terms— dehazing, depth, quantitative evaluation

I. INTRODUCTION

Image dehazing, a typical image enhancement technique studied extensively in the recent years, aims to recover the original light intensity of a hazy scene. While earlier dehazing approaches employ additional information such as multiple images [3] or a rough estimate of the depth [4], recent techniques have tackled this problem by using only the information of a single hazy input image [5], [6], [7], [8], [9], [10], [11], [12], [13], [14], [15], [16]. The existing techniques restore the latent image assuming the physical model of Koschmieder [17]. Since dehazing problem is mathematically ill-posed there are various strategies to estimate the two unknowns: the airlight constant and the transmission map.

Fattal [5] employs a graphical model that solves the ambiguity of airlight color assuming that image shading and scene transmission are locally uncorrelated. Tan's method [6] maximizes local contrast while constraining the image intensity to be less than the global atmospheric light value. He et al. [7], [18] introduce a powerful approach built on the statistical observation of the dark channel, that allows a rough estimation of the transmission map, further refined by an alpha matting strategy [19]. Tarel and Hautière [8] introduce a filtering strategy assuming that the depth-map must be smooth except along edges with large depth jumps. Kratz and Nishino [9] propose a Bayesian probabilistic method that jointly estimates the scene albedo and depth from a single degraded image by fully leveraging their latent statistical structures. Ancuti et al. [10] describe an enhancing technique built on a fast identification of hazy regions based on the *semi-inverse* of the image. Ancuti and Ancuti [12] introduce a multi-scale fusion procedure that restore such hazy image by defining proper inputs and weight maps. The method has been extended recently by Choi et al. [20]. Meng et al. [21] propose a regularization approach based on a novel boundary constraint applied on the transmission map. Fattal [13] presents a method inspired from color-lines, a generic regularity in natural images. Tang et al. [16] describe a framework that learns a set of feature for image dehazing.

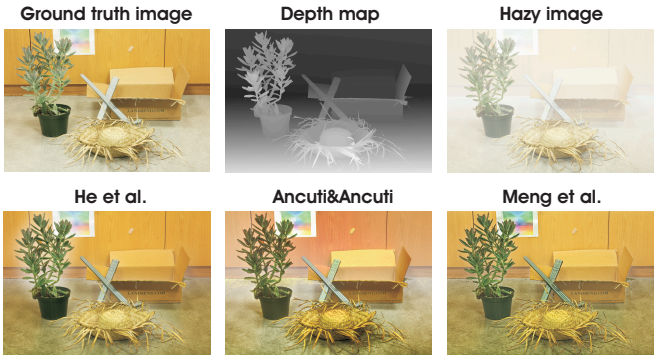

Fig. 1. *D-HAZY dataset provides ground truth images and the corresponding hazy image derived from the depth map (known). In the bottom row are shown results yielded by several recent dehazing techniques [18], [12], [21].*

There have been a few attempts to quantitatively evaluate dehazing methods. All of them have been defined as non-reference image quality assessment (NR-IQA) strategies. Hautiere et al. [22] propose a blind measure based on the ratio between the gradient of the visible edges between the hazy image and the restored version of it. Chen et al. [23] introduce a general framework for quality assessment of different enhancement algorithms, including dehazing methods. Their evaluation was based on a preliminary subjective assessment of a dataset which contains source images in bad visibility and their enhanced images processed by different enhancement algorithms. Moreover, general non reference image quality assessment (NR-IQA) strategies [24], [25], [26] have not been designed and tested for image dehazing.

However, none of these quality assessment approaches have been commonly accepted and as a consequence a reliable data set for dehazing problem is extremely important. Unlike other image enhancing problems for dehazing task capturing a valid ground

Part of this work has been funded by the Belgian NSF, and by a MOVE-IN Louvain, Marie Curie Fellowship.

Part of this work has been funded from Marie Curie Actions of EU-FP7 under REA grant agreement no. 600388 (TECNIOspring programme), and from ACCIO: TECSPR14-2-0023.

truth image is not trivial. The procedure to record both the reference (haze-free) and the hazy image in the same illumination condition is generally intractable. The FRIDA dataset [27] designed for Advanced Driver Assistance Systems (ADAS) is a synthetic image database (computer graphics generated scenes). It contains 66 roads synthesized scenes and besides the reduced level of generality and complexity of the scenes as a computer-generated dataset some parameter settings are not valid for real scenarios.

In this paper we introduce a novel dataset that allows to quantitatively evaluate the existing dehazing techniques. Our dataset contains 1400+ images of real complex scenes. In order to generate the hazy images we use the extended *Middleburry*[1] dataset that contains high quality real scenes and corresponding depth map. Moreover, we improve our dataset using recent *NYU-Depth V2*[2], a large dataset that includes various indoor scenes with RGB and depth maps captured by a Microsoft Kinect sensor. Employing the Koschmieder's physical model [17] of light transmission in hazy scenes, assuming uniform atmospheric intensity and uniform haze density, and using the reference depth map available from the dataset, we are able to synthesize haze in the considered scenes. Even if the strict validity of the Koschmieder model is arguable in arbitrary illumination and haze density conditions, it is revelvant to synthetise hazy images based on this model because it is at the core of all modern dehazing techniques. Hence, all those methods should provide good results when the model is valid. As an important and surprising contribution, our work however reveals that, even for hazy images that perfectly fit the model, none of the existing dehazing technique is able to accurately reconstruct the original image from its hazy version. This observation has been derived from a comprehensive evaluation of several state of the arts dehazing approaches based on SSIM [28] and CIEDE2000 [29] measures computed between the reference (haze-free image) and the restored results produced by different dehazing techniques.

II. FROM DEPTH TO HAZY SCENES

In this section we first describe the optical model assumed for hazy scenes and how we built our hazy dataset following this model.

II-A. Optical Model of Hazy Scenes

A hazy medium is characterized by small particles that respond to changes in relative humidity acting as small droplets nuclei when the humidity is higher than a certain level. In such medium, the light that is passing through it is attenuated along its original course and is distributed to other directions. Mathematically this process is expressed by the the image formation model of Koschmieder's model [17] that is widely accepted by all the recent dehazing approaches. Based on this model, due to the atmospheric particles that absorb and scatter light, only a certain percentage of the reflected light reaches the observer. The light intensity $\mathcal{I}$ of each pixel coordinate x, that passes a hazy medium, is the result of two main additive components - *direct attenuation* $\mathcal{D}$ and *airlight* $\mathcal{A}$:

$$\mathcal{I}(x) = \mathcal{D}(x) + \mathcal{A}(x) = \mathcal{J}(x)\ T(x) + A_\infty\ [1 - T(x)] \quad (1)$$

where $\mathcal{J}$ is the scene radiance of a clear medium (haze-free image), T is the *transmission* along the cone of vision and A_∞ is the atmospheric light (a color constant that is computed globally for the day-time dehazing).

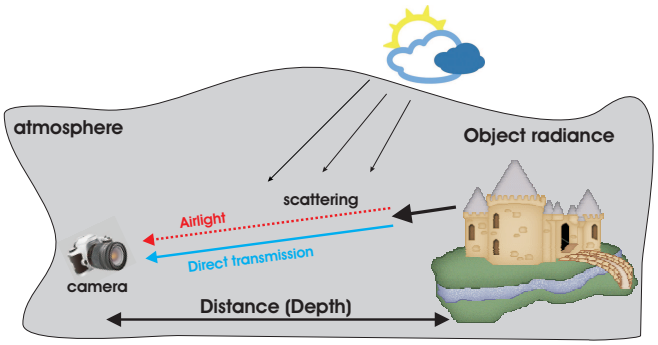

Fig. 2. ***Physical model of a hazy scene.***

The airlight component is linearly correlated with the distance between the observer and the target object of the scene. The first component of the model, *direct attenuation* $\mathcal{D}$, describes how the scene radiance is attenuated with the distance. The second one, the *airlight* component $\mathcal{A}$ represents the principal source of the additive color shifting and is expressed as:

$$\mathcal{A}(x) = A_\infty\ [1 - T(x)] \quad (2)$$

where T is the transmission and represents the relative fraction of light able to cross the hazy medium between the observer and scene surface, without being scattered.

Basically, the transmission map T is directly related with the depth of the scene and considering a homogeneous medium this value is expressed as:

$$T(x) = e^{[-\beta\ d(x)]} \quad (3)$$

where β is the medium attenuation (extinction) coefficient due to the light scattering, while d represents the distance between the observer and the considered surface.

II-B. Using Depth to Synthesize Hazy Scenes

Depth is a key parameter in Equation 3. In general, the existing datasets, are relatively limited in resolution, , realism and accuracy of depth ground truth. To overcome these limitations the recent work of Scharstein et al. [1] has introduced a novel dataset to evaluate stereo algorithms. The dataset is generated using structured light [30]. It represents an extension of the well-known Middlebury dataset and contains 23 images (6-megapixel) of indoor scenes with subpixel-accurate depth ground truth.

To deal withthe the lack of ground truth in occluded regions, for the images of the Middlebury dataset we have employed the recent weighted median filtering strategy introduced by Ma et al. [31].

Additionally, for a more comprehensive evaluation we have also considered the recent NYU-Depth V2 data set [2]. This data set includes various indoor scenes with RGB and depth maps captured by Microsoft Kinect sensor. Missing depth values have been filled in using the colorization scheme of Levin et al. [32]. While this dataset is not as accurate as the Middlebury dataset it has the advantage to be much larger (1449, 640×480 images), with various scenes.

Based on the optical model described above, we synthesize the hazy scenes using the reference (haze-free) image and its

[1] http://vision.middlebury.edu/stereo/data/scenes2014/
[2] http://cs.nyu.edu/~silberman/datasets/nyu_depth_v2.html

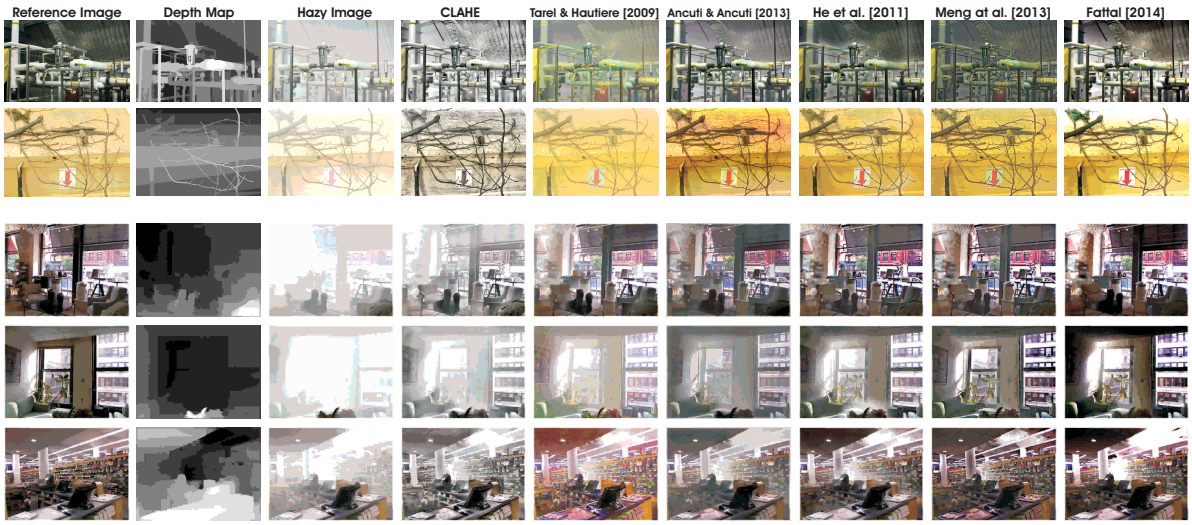

Fig. 3. ***Comparative results.*** *The first two rows show the ground truth, depth map, hazy images and results derived from the Middleburry dataset while the last three rows show results derived from NYU-Depth dataset.*

corresponding depth map. First, for each image, the transmission map is estimated based on equation 3 using the depth d and the medium attenuation coefficient β. β is set by default to 1, which corresponds to moderate and homogenous haze. Additionally, for the atmospheric light constant A_∞ we assume a pure white value [1 1 1], and generate the hazy images based on equations 1 and 3 as:

$$\mathcal{I}(x) = \mathcal{J}(x)\ e^{[-\beta\ d(x)]} + A_\infty\ \left[1 - e^{[-\beta\ d(x)]}\right] \qquad (4)$$

III. EVALUATED TECHNIQUES

In this study, using our new dataset D-HAZY, we evaluate perform an comprehensive validation comparing several state of the art single image dehazing techniques and one well-known enhancing method. For all tested algorithms we use the original implementation provided by the authors. In the following we briefly describe these techniques.

1. Tarel and Hautiere [8] introduce one of the first single dehazing image approach. The method restores the visibility of hazy images based on a filtering strategy. They assumes that the white-balance is performed as a pre-processing step and estimates the transmission as a percentage of the difference between the local average of image and the local standard deviation of it. The transmission is refined based on an extended version of the median filter. The method has the advantage to be fast working for both color and grayscale images.

2. He et al. [7], [18] proposes a novel prior the dark-channel that is derived from the dark object of Chavez [33]. They explore the statistics that in most of the local regions which do not cover the sky, some pixels in general are characterized by very low values in at least one color channel. These filtered pixels per patch are used to estimate the haze transmission that is refined by an alpha matting strategy. In our evaluation we employ the dark channel prior refined based on the guided filter [34].

3. Meng et al. [21] introduce a regularization strategy that explores effectively the boundary constraint on the transmission map. The boundary constraint of the transmission is an extension of the well-known dark channel prior [7]. The transmission is refined by an optimization problem using the boundary constraint combined with a weighted L1-norm based contextual regularization.

4. Ancuti and Ancuti [12] describe an effective a multi-scale fusion strategy for single-image dehazing. They derive two inputs, the first one is processed by white balancing the original hazy image while the second input is obtained by subtracting for each pixel the average luminance value of the entire image. Their important features are filtered by computing several measures (weight maps) that are blend in a multi-scale fusion strategy.

5. Fattal [13] introduces an approach that explores the color lines, pixels of small image patches typically exhibit a one-dimensional distribution in RGB color space. A first estimate of the transmission map is obtained by computing the lines offset from the origin. The final transmission map is produced based on a Markov random field that refines the noise and other artifacts due to the scattering.

6. CLAHE (Contrast-limiting adaptive histogram equalization) [35] is a well-known enhancing technique that restores the contrast of the images. Desighned original for medical imaging CLAHE extends the adaptive histogram equalization (AHE) by applying a contrast limiting procedure. CLAHE splits the images into contextual regions and employs the histogram equalization to each of the region. To generate the CLAHE results we used the original implementation of Matlab2014b.

IV. RESULTS AND DISCUSSION

Qualitatively, as expected, CLAHE [35] yields the less visually compelling results (see Fig. 3). While the method of Tarel and Hautiere [8] has the advantage to be computationally efficient, the

	CLAHE		Tarel		Ancuti&Ancuti		He et al.		Meng et al.		Fattal	
	SSIM	CIEDE2000	SSIM	CIEDE2000	SSIM	CIEDE2000	SSIM	CIEDE2000	SSIM	CIEDE2000	SSIM	CIEDE2000
Adirondack	0.728	11.257	0.851	15.195	0.890	10.820	0.858	10.775	0.882	11.106	0.753	16.057
Backpack	0.610	14.896	0.874	11.721	0.877	11.739	0.916	10.013	0.890	10.629	0.869	13.300
Bicycle1	0.768	18.067	0.876	8.843	0.899	12.669	0.882	15.296	0.766	23.259	0.809	16.448
Cable	0.499	25.054	0.649	26.469	0.617	24.249	0.710	16.379	0.668	18.895	0.743	13.684
Classroom1	0.609	11.205	0.799	23.315	0.886	11.839	0.911	6.315	0.872	9.834	0.870	20.742
Couch	0.613	11.519	0.716	25.640	0.854	13.262	0.908	6.736	0.862	10.775	0.779	22.941
Flowers	0.703	16.910	0.792	15.861	0.816	14.618	0.876	8.646	0.829	14.013	0.876	8.703
Jadeplant	0.549	26.364	0.687	20.187	0.632	28.415	0.689	19.223	0.699	21.418	0.631	32.390
Mask	0.682	14.781	0.875	11.754	0.860	11.603	0.888	9.703	0.828	14.875	0.886	11.823
Motorcycle	0.761	13.026	0.760	18.585	0.825	14.486	0.816	13.706	0.805	14.150	0.760	17.858
Piano	0.699	9.757	0.790	20.301	0.839	10.336	0.888	6.177	0.855	8.861	0.794	12.588
Pipes	0.628	16.898	0.678	24.285	0.715	19.193	0.779	9.643	0.751	11.541	0.681	15.463
Playroom	0.672	11.952	0.792	18.367	0.831	13.233	0.878	7.430	0.822	12.070	0.802	16.091
Playtable	0.717	9.418	0.831	19.060	0.842	9.118	0.907	8.028	0.865	14.119	0.813	11.519
Recycle	0.688	13.400	0.895	11.890	0.898	12.474	0.876	14.964	0.871	14.846	0.727	20.655
Shelves	0.754	7.681	0.883	15.202	0.929	7.181	0.890	11.649	0.889	14.413	0.871	12.400
Shopvac	0.669	17.659	0.726	29.251	0.788	19.268	0.827	16.287	0.821	17.569	0.758	32.504
Sticks	0.715	20.073	0.884	8.489	0.852	15.214	0.948	7.213	0.953	8.196	0.921	10.865
Storage	0.692	13.335	0.853	16.636	0.806	14.782	0.883	10.194	0.870	12.086	0.819	16.851
Sword1	0.607	20.070	0.862	12.097	0.835	14.809	0.910	9.660	0.892	10.436	0.865	13.822
Sword2	0.638	12.184	0.872	13.485	0.887	12.051	0.899	12.458	0.849	15.494	0.758	37.965
Umbrella	0.574	20.371	0.818	15.130	0.837	15.933	0.838	20.229	0.798	21.489	0.659	33.149
Vintage	0.711	14.907	0.858	8.236	0.856	14.612	0.917	10.049	0.780	21.796	0.858	15.794
Average	0.665	15.252	0.810	16.956	0.829	14.431	0.865	11.338	0.831	14.429	0.796	18.418

Table I. ***Quantitative evaluation.*** *For each image derived from the Middleburry dataset we compute the SSIM and CIEDE2000 indexes between the ground truth images and the enhanced results of the evaluated techniques.*

results produced by this method look over-saturated with unpleasing halo artifacts. Guided by several perceptual measures the method of Ancuti and Ancuti [12] mitigates the introduction of structural artifacts due to the multi-scale fusion strategy. Despite of its euristic built-in concept, the method of He et al. [7] appears to perform generally better than the other approaches both in color and structure restoration. However, it can be observed that this approach yields over-corrected results in white and gray regions where no color channel is dominant. Since it also builds on the dark channel prior, it is not surprising to observe that the approach of Meng et al. [21] yields similar results as He et al. [7], with slightly reduced artifacts, thanks to high-order filtering of the transmission map. Whilst being quite effective on some images, the technique of Fattal [13] regularly over-saturates some regions due to the color-lines prior, and sometimes introduces unpleasing structural artifacts around the edges.

Quantitatively, to validate the different techniques described previously, we compare their outcome with the ground truth haze-free images provided of the D-HAZY dataset. Since PSNR has been proven to not be very effective in predicting human visual response to image quality [28], we compute the well-known structural similarity (SSIM) index [36] that compares local patterns of pixel intensities that have been normalized for luminance and contrast. SSIM index yields decimal values between -1 and 1, with maximum value 1 for two identical images.

Moreover, because in image dehazing restoration of the color is crucial and cannot be evaluated reliably by SSIM we employ an additional evaluation metric. The difference between two colors is a metric of high interest in color science. While the earlier measures (e.g. CIE76 and CIE94) shown important limitations to resolve the perceptual uniformity issue, CIE introduced CIEDE2000 [29], [37] which defines a more complex, yet most accurate color difference algorithm. CIEDE2000 yields values in the range [0,100] with smaller values indicating better color preservation, and values less than 1 corresponding to visually imperceptible differences.

Table I presents a detailed validation for the 23 Middleburry dataset images and table II shows the average values of SSIM and CIEDE2000 measured over the 1449 NYU-Depth images.

From these tables, we conclude that the method of He et al. [7] performs the best in average. A second group of methods including Meng et al. [21], Ancuti and Ancuti [12] and Fattal [13], perform relatively well both in terms of structure and color restoration.

	CLAHE	Tarel	Ancuti	He	Meng	Fattal
SSIM	0.622	0.719	0.771	0.811	0.773	0.747
CIEDE2000	18.054	17.742	14.136	11.029	12.216	14.656

Table II. *Quantitative evaluation of the 1449 images generated based on the NYU-Depth dataset. In this table are shown the average values of the SSIM and CIEDE2000 indexes over the entire dataset (1449 images).*

In general, all the tested methods introduce structural distortions such as halo artifacts close to the edges, that are amplified in the faraway regions. Moreover, due to the poor estimation of the airlight and transmission map from the hazy image, some color distortions may create some unnatural appearance of the restored images. In summary, there is not a single technique that performs the best for all images. The relatively low values of SSIM and CIEDE2000 measures prove once again the difficulty of single image dehazing task and the fact there is still much room for improvement.

V. REFERENCES

[1] D. Scharstein, H. Hirschmller, Y. Kitajima, G. Krathwohl, N. Nesic, X. Wang, and P. Westling, "High-resolution stereo datasets with subpixel-accurate ground truth.," *In German Conference on Pattern Recognition*, 2014.

[2] Pushmeet Kohli Nathan Silberman, Derek Hoiem and Rob Fergus, "Indoor segmentation and support inference from rgbd images," in *ECCV*, 2012.

[3] S.G. Narasimhan and S.K. Nayar, "Contrast restoration of weather degraded images," *IEEE Trans. on Pattern Analysis and Machine Intell.*, 2003.

[4] J. Kopf, B. Neubert, B. Chen, M. Cohen, D. Cohen-Or, O. Deussen, M. Uyttendaele, and D. Lischinski, "Deep photo: Model-based photograph enhancement and viewing," in *Siggraph ASIA, ACM Trans. on Graph.*, 2008.

[5] Raanan Fattal, "Single image dehazing," *SIGGRAPH*, 2008.

[6] Robby T. Tan, "Visibility in bad weather from a single image," *In IEEE Conference on Computer Vision and Pattern Recognition*, 2008.

[7] K. He, J. Sun, and X. Tang, "Single image haze removal using dark channel prior," *In IEEE CVPR*, 2009.

[8] J.-P. Tarel and N. Hautiere, "Fast visibility restoration from a single color or gray level image," *In IEEE ICCV*, 2009.

[9] L. Kratz and K. Nishino, "Factorizing scene albedo and depth from a single foggy image," *ICCV*, 2009.

[10] C. O. Ancuti, C. Ancuti, C. Hermans, and P. Bekaert, "A fast semi-inverse approach to detect and remove the haze from a single image," *ACCV*, 2010.

[11] C. O. Ancuti, C. Ancuti, and P. Bekaert, "Effective single-image dehazing by fusion," in *In IEEE ICIP*, 2010.

[12] C.O. Ancuti and C. Ancuti, "Single image dehazing by multi-scale fusion," *IEEE Transactions on Image Processing*, vol. 22(8), pp. 3271–3282, 2013.

[13] Raanan Fattal, "Dehazing using color-lines," *ACM Trans. on Graph.*, 2014.

[14] C. Ancuti and C. O. Ancuti, "Effective contrast-based dehazing for robust image matching," *IEEE Geoscience and Remote Sensing Letters*, 2014.

[15] S. Emberton, L. Chittka, and A. Cavallaro, "Hierarchical rank-based veiling light estimation for underwater dehazing," *Proc. of British Machine Vision Conference (BMVC)*, 2015.

[16] K. Tang, J. Yang, and J. Wang, "Investigating haze-relevant features in a learning framework for image dehazing," *In IEEE Conference on Computer Vision and Pattern Recognition*, 2014.

[17] H. Koschmieder, "Theorie der horizontalen sichtweite," in *Beitrage zur Physik der freien Atmosphare*, 1924.

[18] K. He, J. Sun, and X. Tang, "Single image haze removal using dark channel prior," *IEEE Trans. on Pattern Analysis and Machine Intell.*, 2011.

[19] A. Levin, D. Lischinski, and Y. Weiss, "A closed form solution to natural image matting," *In IEEE Transactions on Pattern Analysis and Machine Intelligence (TPAMI)*, 2008.

[20] L. K. Choi, J. You, and A. C. Bovik, "Referenceless prediction of perceptual fog density and perceptual image defogging," *In IEEE Trans. on Image Processing*, 2015.

[21] G. Meng, Y. Wang, J. Duan, S. Xiang, and C. Pan, "Efficient image dehazing with boundary constraint and contextual regularization," *In IEEE Int. Conf. on Computer Vision*, 2013.

[22] N. Hautiere, J.-P. Tarel, D. Aubert, and E. Dumont, "Blind contrast enhancement assessment by gradient ratioing at visible edges," *Journal of Image Analysis and Stereology*, 2008.

[23] Z. Chen, T. Jiang, and Y. Tian, "Quality assessment for comparing image enhancement algorithms," *In IEEE Conference on Computer Vision and Pattern Recognition*, 2014.

[24] A. Mittal, A. K. Moorthy, and A. C. Bovik, "No-reference image quality assessment in the spatial domain," *In IEEE Trans. on Image Processing*, 2012.

[25] A. Mittal, R. Soundararajan, and A. C. Bovik, "Making a completely blind image quality analyzer," *In IEEE Signal Processing Letters*, 2013.

[26] M. A. Saad, A. C. Bovik, and C. Charrier, "Blind image quality assessment: A natural scene statistics approach in the dct domain," *In IEEE Trans. on Image Processing*, 2012.

[27] J.-P. Tarel, N. Hautire, L. Caraffa, A. Cord, H. Halmaoui, and D. Gruyer, "Vision enhancement in homogeneous and heterogeneous fog," *IEEE Intelligent Transportation Systems Magazine*, 2012.

[28] Z. Wang and A. C. Bovik, "Modern image quality assessment," *Morgan and Claypool Publishers*, 2006.

[29] G. Sharma, W. Wu, and E. Dalal, "The ciede2000 color-difference formula: Implementation notes, supplementary test data, and mathematical observations," *Color Research and Applications*, 2005.

[30] D. Scharstein and R. Szeliski, "High-accuracy stereo depth maps using structured light.," *In IEEE Conference on Computer Vision and Pattern Recognition*, 2003.

[31] Z. Ma, K. He, Y. Wei, J. Sun, and E. Wu, "Constant time weighted median filtering for stereo matching and beyond," *International Conference on Computer Vision*, 2013.

[32] A. Levin, D. Lischinski, and Y. Weiss, "Colorization using optimization," *In SIGGRAPH*, 2004.

[33] P.S. Chavez, "An improved dark-object subtraction technique for atmospheric scattering correction of multispectral data," *Remote Sensing of Environment*, 1988.

[34] K. He, J. Sun, and X. Tang, "Guided image filtering," *In IEEE Transactions on Pattern Analysis and Machine Intelligence (TPAMI)*, 2013.

[35] K. Zuiderveld, "Contrast limited adaptive histogram equalization," *Graphics Gems IV*, 1994.

[36] Z. Wang, A. C. Bovik, H. R. Sheikh, and E. P. Simoncelli, "Image quality assessment: From error visibility to structural similarity," *IEEE Transactions on Image Processing*, 2004.

[37] S. Westland, C. Ripamonti, and V. Cheung, "Computational colour science using matlab, 2nd edition," *Wiley*, 2005.